Hindawi
International Journal of Antennas and Propagation
Volume 2022, Article ID 1958247, 17 pages
https://doi.org/10.1155/2022/1958247

Research Article

Multi-Band mm-Wave Wearable Antenna Synthesized with a Genetic Algorithm

Arebu Dejen,[1] **Murad Ridwan**,[1] **Jeevani Jayasinghe**,[2] **and Jaume Anguera**[3,4]

[1]*School of Electrical and Computer Engineering, AAIT, Addis Ababa University, Addis Ababa, Ethiopia*
[2]*Department of Electronics, Wayamba University of Sri Lanka, Kuliyapitiya, Sri Lanka*
[3]*Telecommunication Engineering, University at Ramon Llull, Barcelona, Spain*
[4]*Ignion, Barcelona, Spain*

Correspondence should be addressed to Arebu Dejen; arbdjn@gmail.com

Received 7 April 2022; Revised 4 May 2022; Accepted 5 May 2022; Published 31 May 2022

Academic Editor: Eng Hock Lim

This paper presents the design of a novel fabric-based multi-band microstrip antenna in mm-wave frequencies for wearable applications. The reference patch antenna was etched on a flexible polytetrafluoroethylene (PTFE) fabric substrate with an overall dimension of 18 mm × 18 mm × 0.6 mm and optimized the patch geometry using a binary-coded genetic algorithm. The algorithm iteratively creates a new shape of the path surface, evaluates the cost function, and returns the best-fitted geometry based on the formulated fitness function. The free space and on-body simulation of the best-fitted antenna performance parameter was investigated and analyzed. In free space, the proposed antenna is resonant at five distinct frequencies: 27.8 GHz, 30.3 GHz, 40.1 GHz, 47.2 GHz, and 56.7 GHz. The antenna achieves a wide bandwidth of 0.69, 2.32, 2.22, 1.76, and 8.11 GHz and an improved broadside directivity of 10.3, 8.5, 7.8, 9.6, and 8.9 dB in free space, respectively. For on-body analysis, the antenna was simulated using a three-layer human body phantom model at three distinct distances. The gain and radiation efficiency were significantly reduced when the antenna was close to the phantom model and gradually enhanced as the gap increased. Moreover, the antenna performances were evaluated and compared by using four additional fabric substrates. Because of its excellent on-body performance with flexible textile-based substrates, the optimized antenna is a suitable candidate for multi-band body-centric communications.

1. Introduction

In recent years, there have been a number of investigations on wireless monitoring of human attributes. Several services are anticipated from wearable devices addressing the ever-growing customer requirements. Designers and researchers in the field of wearable antennas continue exploiting antenna technology to meet client needs. Globally, extensive researches have undertaken towards innovative and tiny wearable antennas capable of wirelessly communicating human body parameters to a nearby accessible network. As wearable antenna technology advances, new and diverse applications such as medical monitoring, smart diagnosis, aging care, battle-field personal care, astronaut monitoring, child protection, and location-based services have emerged [1]. Such devices are used in sports medicine to track the characteristics of athletes in training. Wearable antennas are often employed in hazardous areas to manage the work environment [2]. The wearable antenna in a well-designed system has appropriate operating bandwidth, acceptable radiation characteristics for human tissue, and high enough gain and directivity to suit the requirements. The antenna, on the other hand, must be light, flexible, compact in size, inexpensive, resistant to damage, and comfortable to wear. Microstrip antennas are an attractive option for mm-wave multi-band wearable antennas. Even though the microstrip antenna has low gain and narrow bandwidth with some other deficiencies in its performance, the antenna is advantageous over other antennas due to its low profile, easy manufacturing, and planar structure.

The dynamic development of wireless communication derives coexisted multiple standards that increase the demand for multi-functional antennas. Because of the large bandwidth available at mm-wave frequency, numerous applications such as wireless networks, mobile communication, internet of things, wireless human monitoring systems, and machine-to-machine communications will be facilitated and become more prevalent in the band for the next-generation technologies. In the case of human monitoring systems, networks in the band are critical because they allow data transmission over small ranges of cellular systems. The mm-wave band is part of the radio frequency spectrum between 30 and 300 GHz, corresponding to a free space wavelength ranging from 10 to 1 mm. As the photon energy is insufficient to take an electron from an atom, the radiation from this band is not ionized. Instead, the absorption of electromagnetic mm-wave energy by tissues results in the primary physiologic consequence of heat [3]. Thus, antennas in mm-wave for a body-centric network should be optimized according to the rules and guidelines of specific absorption rate (SAR) to protect the human tissue from injuries.

FCC allocates the following mm-wave bands for wireless applications: 24–40 GHz for 5G cellular communication, 33.4–36 GHz for vehicle speed detection, 57–59 GHz for meteorological applications, and 57–66 GHz for WPAN [4, 5]. Although mm-wave signals face several propagation obstacles, multi-band antennas for wearable devices operating at these frequencies are critical for enhancing communication capabilities with a variety of wireless protocols. The combination of automated optimization algorithms and electromagnetic analysis tools was employed to meet the complex design criteria of the wearable multi-band microstrip antennas at mm-wave frequency. Several approaches and optimization algorithms have been used in the literature to improve multi-band and performance of microstrip antennas. Employing slits and slots on the antenna structure was presented in [6]. Loading a metamaterial structure as part of the microstrip antenna is also reported [7, 9].

An antenna designed using theoretically derived parameters does not provide sufficient performance to meet real-world communication requirements. It is a complex and time-consuming procedure to find the parameters of any antenna using simple intuition, experience, and practical measurements. Desired performance, such as multi-band operation, adequate bandwidth, and good gain, can be achieved by tuning optimum design parameters and geometries using autonomous algorithms. Optimization algorithms such as a genetic algorithm (GA) [10], ant colony optimization [11], simulated annealing algorithm, particle swarm optimization [12], differential evolution [13], bacteria foraging optimization [14], and many others can be used to optimize the design parameters of the antenna. In electromagnetic problems, a far-field simulation is required to estimate the cost function, which is time-consuming. Considering a limited computing budget, algorithms that do not require derivatives knowledge of the objective function are advantageous. Other considerations to consider while choosing a better algorithm are computational effectiveness, solution quality, convergence, and optimization accuracy. In antenna optimization, the genetic algorithm surpasses the other methods in terms of intended outputs [15].

This paper presents a wearable multi-band mm-wave microstrip antenna using a binary-coded genetic algorithm for the wireless human monitoring system. For operational reasons, antennas of this type should use fabric substrates for easy integration with clothes [16]. Simultaneously, the bandwidth of such an antenna should be as broad as possible to allow for abundant data transfer in the link in all operating bands. The radiating patch shape was divided into smaller rectangular cells and assigned a binary "0" for nonconducting cells and a binary "1" for conducting cells on the patch surface to attain optimization. The iterative "on" and "off" features of radiating surface always try a new patch geometry model and evaluate the fitness function until the fit individual appears [17]. The paper uses MATLAB and HFSS software in combination for iterative simulation. The MATLAB software was used to generate the VBS files with the modeled antenna details. HFSS calls the VBS file, simulates the antenna, and exports the resulting performance to the genetic algorithm optimizer into the primary function in MATLAB.

2. Genetic Algorithm (GA)

A genetic algorithm is an evolutionary search algorithm based on the heredity of the individual. The algorithm evaluates the cost function and selects the best-fitted individuals for reproduction. The first generation of the population produces randomly, and the rest generations generate through reproduction. The different operators of GA are responsible for the optimum design of the antenna through selection based on the formulated suitable fitness function. Crossover, mutation, and selection are the genetic operators that allow reproduction. The crossover operator reproduces a diverse population. Mutation adds a degree of diversity to the population to protect it from premature convergence [18]. In antenna optimization, GA employed to improve the directivity [19], multi-functionality [20], bandwidth [21], and size reduction [22] of antenna. It optimized the antenna's dimensions, the feeding point's position, the position and size of slots on antenna structure, and the position of shorting pins for appropriate propagation and resonance.

When using GA for antenna optimization to meet a specific performance goal, the optimizer and antenna structure code must be correctly programmed and interfaced. When the structure code is executed, a new antenna model iteratively appears with its recent performance in the optimization process. In each iteration, the GA optimizer begins to evaluate the fitness of each new antenna geometry, and lastly, it provides the best-fitted model with the corresponding performance parameters. The integration of GA computing code for antenna optimization using MATLAB and HFSS interface is presented in Figure 1.

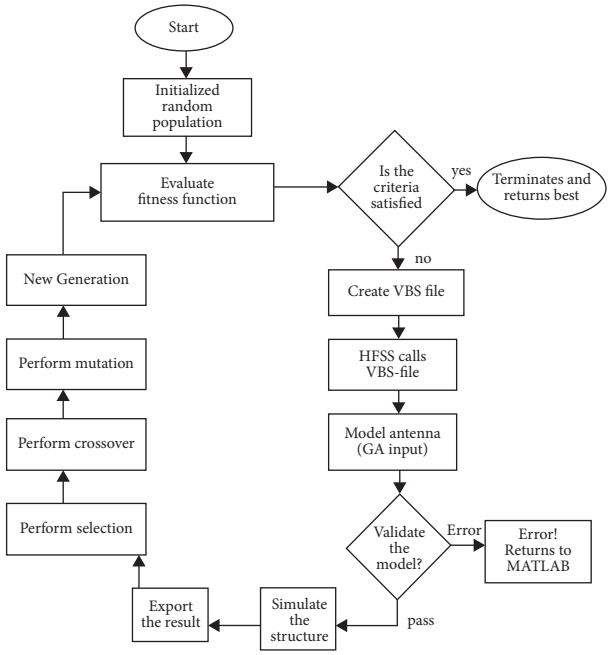

Figure 1: Genetic algorithm flow chart for antenna optimization.

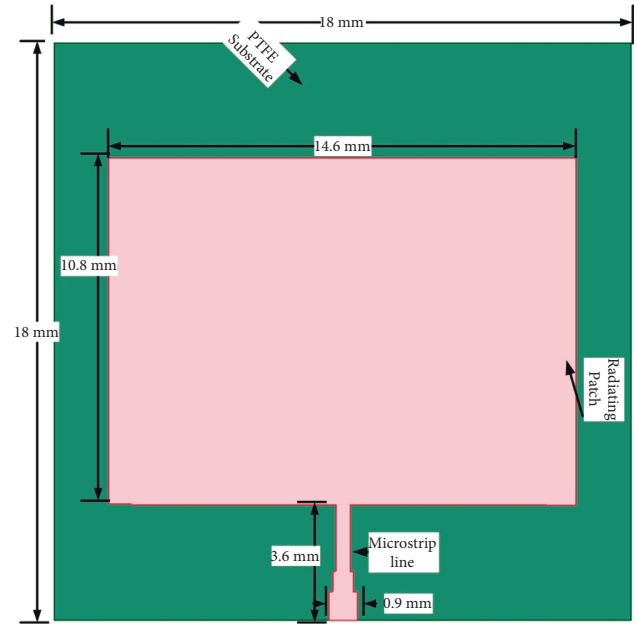

Figure 2: Proposed reference microstrip antenna model on the finite ground plane.

3. Antenna Configuration

An appropriate wearable antenna design should be considered to minimize losses in wearable scenarios. The geometric configuration of the reference rectangular microstrip antenna suitable for GA optimization is illustrated in Figure 2. The antenna's radiating patch and ground plane are composed of a 0.035 mm thick perfect electric conductor (PEC). A 0.6 mm thick fabric polytetrafluoroethylene (PTFE) substrate with a dielectric constant of 2.05 and loss tangent of 0.0017 is employed. It is advantageous to minimize the surface wave losses by utilizing a substrate with a low dielectric constant, which simultaneously enhances impedance bandwidth [23]. The overall dimension of the textile substrate is $18 \times 18 \times 0.6\,\text{mm}^3$. The antenna's radiating patch is 10.8 mm × 14.6 mm in size and is fed by a 50 Ω microstrip line that is 3.6 mm long and 0.9 mm wide. Besides the standard procedures in [24] used to calculate antenna dimensions, the parametric analysis was utilized to articulate the patch dimensions in the interest of appropriate reference antenna performance at 39.5 GHz center frequency [25]. The antenna was modeled and simulated using High-Frequency Structure Simulator (HFSS) software. The dimensions of the reference model are summarized in Table 1.

Table 1: Summary of dimensions for the referenced antenna model.

Parameter	Substrate	Patch	Feedline
Length (mm)	18	10.8	3.6
Width (mm)	18	14.6	0.9
Thickness (mm)	0.6	0.035	0.035

4. Optimization Procedure

In this article, GA optimization is used to optimize the patch geometry. In the proposed solution space, the radiating patch geometry has a variety of shapes, and only a few of these configurations perform well. The GA is greedy since it continually seeks the best-fitting individual to ensure the continuation of the generation. In this optimization problem, the surface of the patch is gridded into 8×8 small rectangular cells having the size of $1.3 \times 1.82\,\text{mm}^2$ as shown in Figure 3. When using a binary-coded genetic algorithm, it is evident that 2^{64} unique candidates are available in the solution space. Every rectangular cell on the surface has its corresponding conducting and nonconducting properties. The conducting cells are assigned by gene "1"; on the other hand, the nonconducting property of the cell is represented by gene "0." Each candidate in the problem space has a distinctive value of fitness value. During the "on" and "off" stages of the cell, vertical overlapping was employed to protect the infinitesimal connection between cells on the patch surface [26]. The geometry of the patch surface is varied in each iteration, resulting in a new antenna with a new fitness value for each. Therefore, the performance of the antenna is updated.

The crucial role in the GA optimization process is the formulation of a good fitness function while considering the desired performance criteria. This work formulated the fitness function considering all the performance factors and their target values. The primary goal is to develop a multiband mm-wave microstrip antenna that can operate at five unique frequencies with broad bandwidth for wearable devices. As a result, the fitness function is designed to minimize the reflection coefficient and increase the antenna's working bandwidth. The maximum bandwidth in a single band is fixed to 8 GHz to reduce the computational time while avoiding premature convergence. The weighting

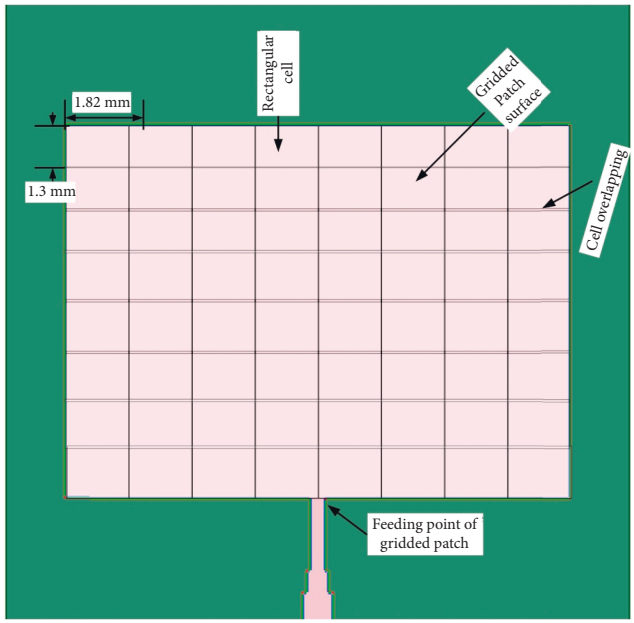

FIGURE 3: Division of patch surface for binary-coded genetic algorithm.

coefficient (C_k) will modify the predicted bandwidth in every five distinct bands: 27.5–28.5 GHz, 29.0–31.5 GHz, 38.5–40.5 GHz, 46.5–48.0 GHz, and 54.0–62.0 GHz. The formulated fitness function is presented in the following equations:

$$\text{Fitness Function} = \sum_{k=1}^{M} \left(C_k Bw(k) - \frac{1}{N} \sum_{i=1}^{N} \rho(f_i) \right), \quad (1)$$

where $\rho(f_i)$ is designed as

$$\rho(f_i) = \begin{cases} \rho(f_i), & \text{if } \rho(f_i) \geq -10\,\text{dB}, \\ -10\,\text{dB}, & \text{if } \rho(f_i) < -10\,\text{dB}, \end{cases} \quad (2)$$

and $Bw(k)$ is designed as

$$Bw(k) = \begin{cases} B(k), & \text{if } B(k) \leq 8\,\text{GHz}, \\ 8\,\text{GHz}, & \text{if } B(k) > 8\,\text{GHz}, \end{cases} \quad (3)$$

where N is the number of sampling frequencies in a given band and M is the number of the operating band. The sampling frequency (f_i) is in the 50 MHz used with the analysis sweep, and $\rho(f_i)$ is the reflection coefficient value in dB at each sampling frequency. C_k assigns the k^{th} bandwidth weighting factor, and $Bw(k)$ is bandwidth at the k^{th} band in GHz.

The patch surface of the reference model is optimized using the following algorithm configurations. The total number of population clusters in a particular generation is 15 individuals. In a population, a single chromosome is represented by 64 genes. Single-point crossover with a probability of 0.8 and single-bit mutation with a mutation rate of 0.01 were used. Throughout 250 generations, the selection operator employed the tournament selection approach.

5. Results and Discussion

The optimization and simulation of the proposed pentaband antenna were carried out utilizing commercially available electromagnetic simulation software HFSS in combination with MATLAB. The geometry of the shape was optimized by providing "on" and "off" states for the rectangular cells on the patch surface until the final structure was obtained using a binary-coded genetic algorithm. The total computing performance of the multi-iterative optimization approach is influenced by the time required for electromagnetic simulation. GA returns the most robust solution out of the $2^{64} = 1.84 \times 10^{19}$ solution space in only 4.3 days at the 250 generations using core I7, 8 GB RAM, and 2.7 GHz processor speed, as shown in Figure 4(a). If we think for a second for each aspirant solution, the computation time would be 5.85×10^{11} years. Hence, GA started to converge after 103 generations, as shown in Figure 4(b).

5.1. Free Space Simulation. The optimized antenna with a fabric PTFE substrate was simulated in free space. The simulated S_{11} curve for both the reference and optimized antennas is presented in Figure 5. The figure demonstrated that the reference model resonated only at a single frequency of 39.5 GHz, with a minimum peak S_{11} value of −20.6 dB. However, the optimized antenna resonates at five distinct bands with center frequencies of 27.8 GHz, 30.3 GHz, 40.1 GHz, 47.2 GHz, and 56.7 GHz and peaks S_{11} values of −34.5 dB, −20.1 dB, −35.2 dB, −22.4 dB, and −25.8 dB, respectively. The VSWR was determined to be less than 2 for all five operational bands, indicating that the proposed antenna was well matched to a 50 Ω microstrip line that transmits the maximum power between the feedline and antenna.

The bandwidth of the reference model is 0.9 GHz since it operates in the range of 39.0–39.9 GHz when $S_{11} < -10$ dB is considered. However, the optimized antenna achieved a better bandwidth in all five operating bands: 0.69 GHz (27.43–28.12 GHz), 2.32 GHz (28.94–31.26 GHz), 2.22 GHz (39.27–41.49 GHz), 1.76 GHz (46.44–48.2 GHz), and 8.92 GHz (53.83–61.94 GHz). The total bandwidth of the antenna is above 15.1 GHz in the operating bands. The bandwidth improvement was made by employing GA optimization.

The 3D gain pattern of the optimized antenna at all five resonant frequencies is presented in Figure 6. The antenna has achieved gain values of 10.2 dB, 8.4 dB, 7.7 dB, 9.5 dB, and 8.4 dB at resonating frequencies of 27.8 GHz, 30.3 GHz, 40.1 GHz, 47.2 GHz, and 56.7 GHz, respectively. As seen from the 3D pattern, they are almost in the broadside direction with slight distortions in higher frequency bands.

5.2. Simulation of the Optimized Antenna on Other Fabric Substrates. For further analysis and investigation of the improved antenna's performance, the free space simulation was carried out by substituting the PTFE substrate with various textiles. Polyester, silk, jeans, and cotton fabrics were

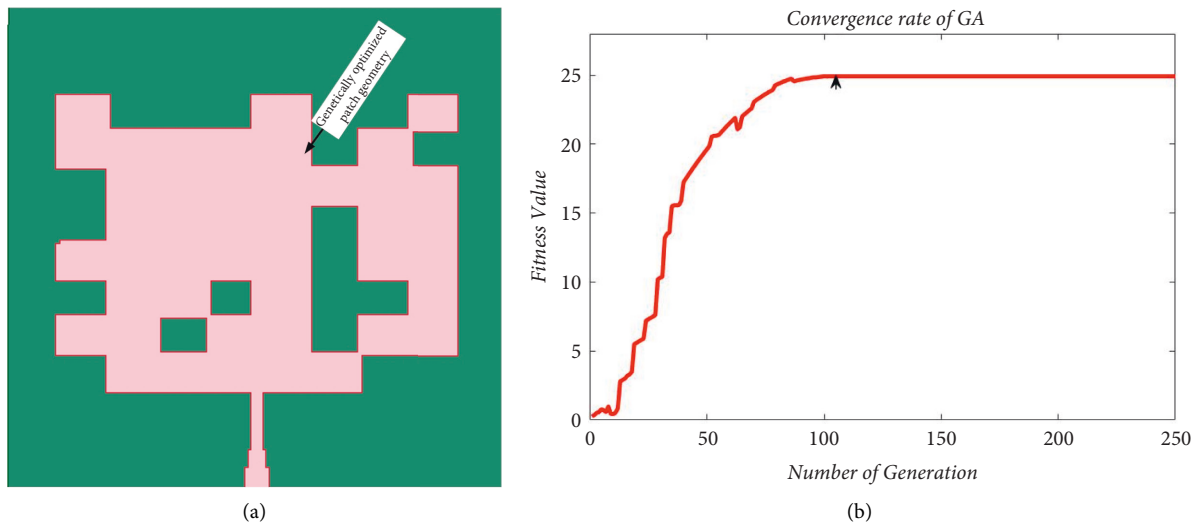

Figure 4: (a) The fitted genetically optimized patch geometry and (b) fitness value versus the number of generations.

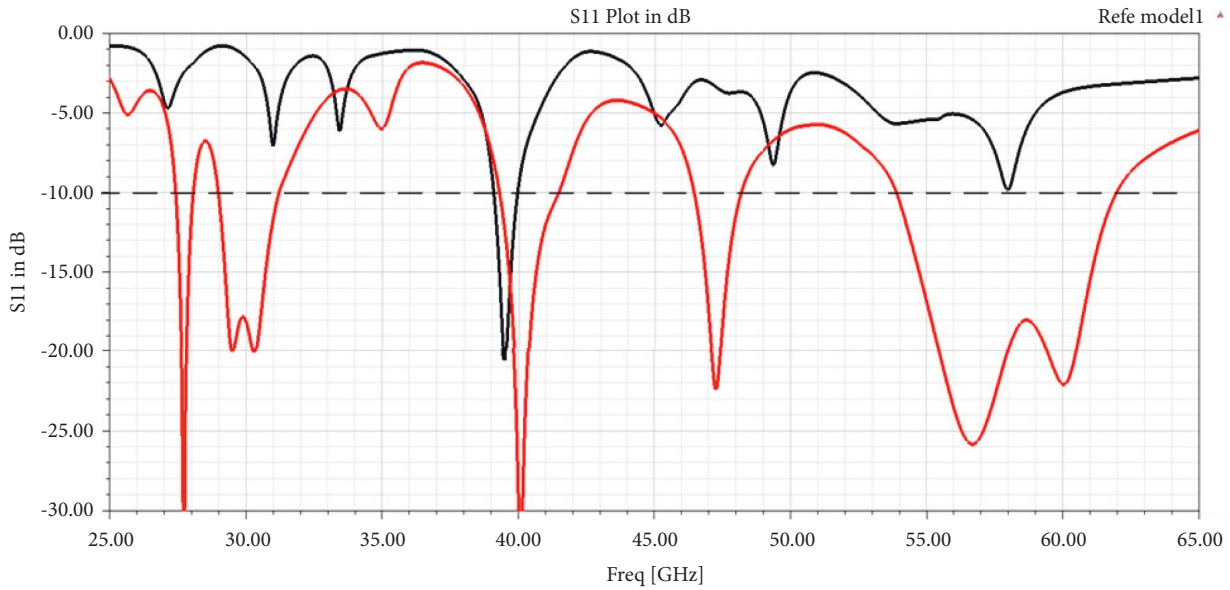

Figure 5: S_{11} curve for the genetically optimized antenna and the reference antenna.

used as substrates with dimensions similar to PTFE. The dielectric constant and tangent loss parameters of fabric substrates are described in Table 2. Figure 7 displays the simulation result of their S_{11} values. The results indicate that the optimized antenna operates in five frequency bands for all fabric substrates. When the dielectric constant decreases, the resonant frequency slightly shifts towards a higher frequency, and the total operating bandwidth of the antenna increases. The cotton-based optimized antenna has a bandwidth of 3 GHz more than the PTFE antenna. Polyester substrate performs closely to the initial PTFE optimized antenna due to the closer dielectric constants. According to simulation results, all of the evaluated substrates exhibited a gain of higher than 8 dB in each band. Table 3 summarizes the free space performance study of the improved antenna with various fabric substrates and the performance of the reference model.

Figures 8 and 9 depict the optimized antenna's gain pattern in E and H plane with various fabric substrates, respectively. The gain patterns of the E and H planes exhibit only slight differences. The patterns guided in the broadside direction show a significant distortion at a few angles, particularly at higher frequencies.

Figures 10(a)–10(e) depict surface current distributions at resonance frequencies to highlight the electromagnetic radiation properties of the optimized antenna in the operating bands. When the proposed antenna operates at resonance frequencies, a significant surface current density was

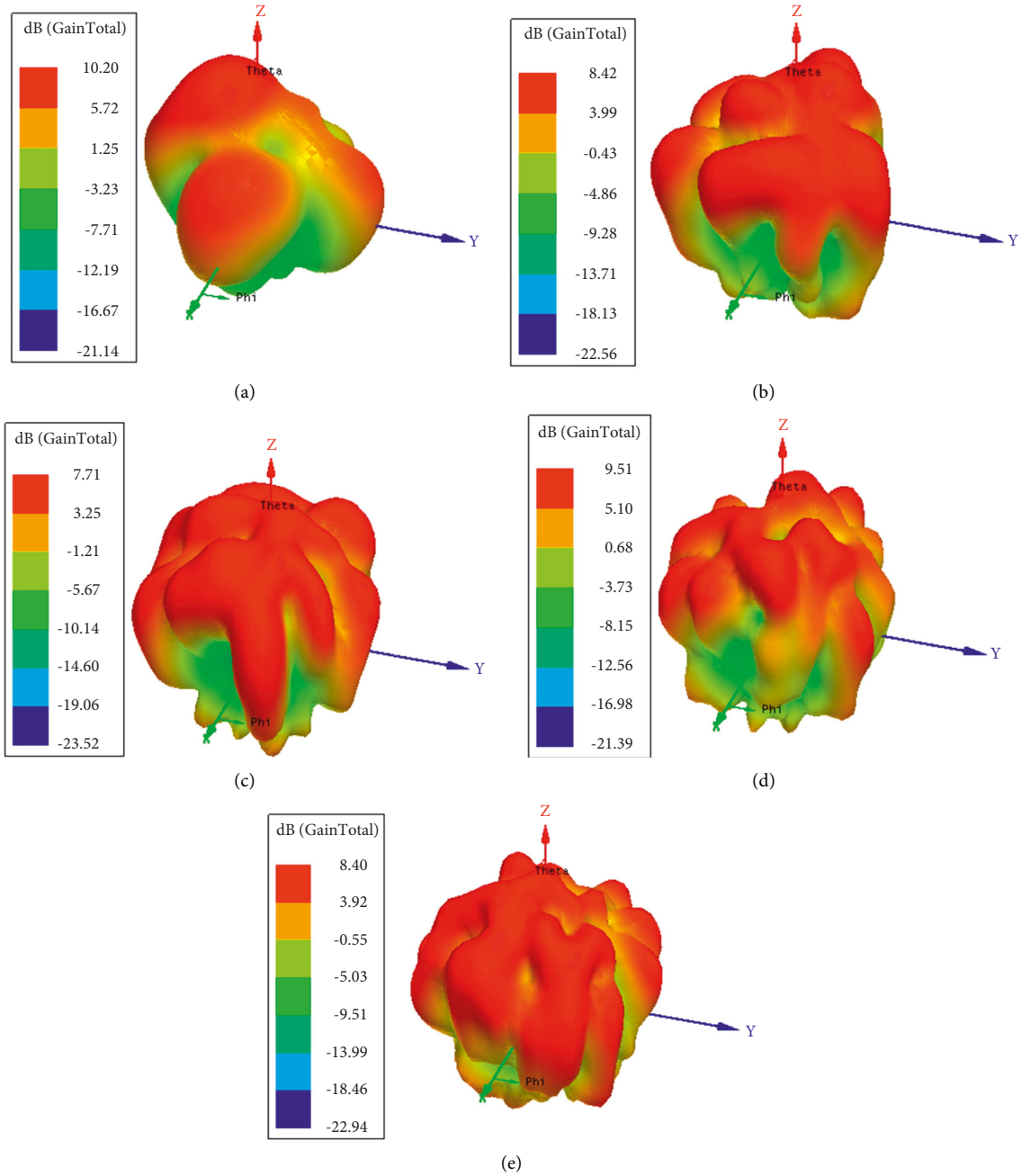

Figure 6: The 3D gain of the optimized antenna at all five resonance frequencies: (a) 27.8 GHz, (b) 30.3 GHz, (c) 40.1 GHz, (d) 47.2 GHz, and (e) 56.7 GHz.

Table 2: The dielectric constant and the loss tangent value of the selected fabric substrates.

No.	Textile material	Dielectric constant	Loss tangent
1	Cotton	1.6	0.04
2	Polyester	1.9	0.0045
3	Jeans	1.67	0.073
4	Silk	1.75	0.012

observed at the junction of the feedline and the patch, as well as a moderate current distribution over the surface of each active rectangular cell.

5.3. On-Body Simulation. In the case of wearable contrivances, the antenna should be simulated conjointly with the proximity of the human body model. The human body model should be discretized into small resolution during the joint simulation. The computational time and memory requirement are high when the model's size is much larger than that of the operating wavelength. As mm-wave signals cannot penetrate human skin more than 0.5 mm, most research studies employ a three-layer phantom representation [26–28]. The heterogeneous and lossy nature of the human body has a direct influence on the antenna performance when it works nearby. A three-

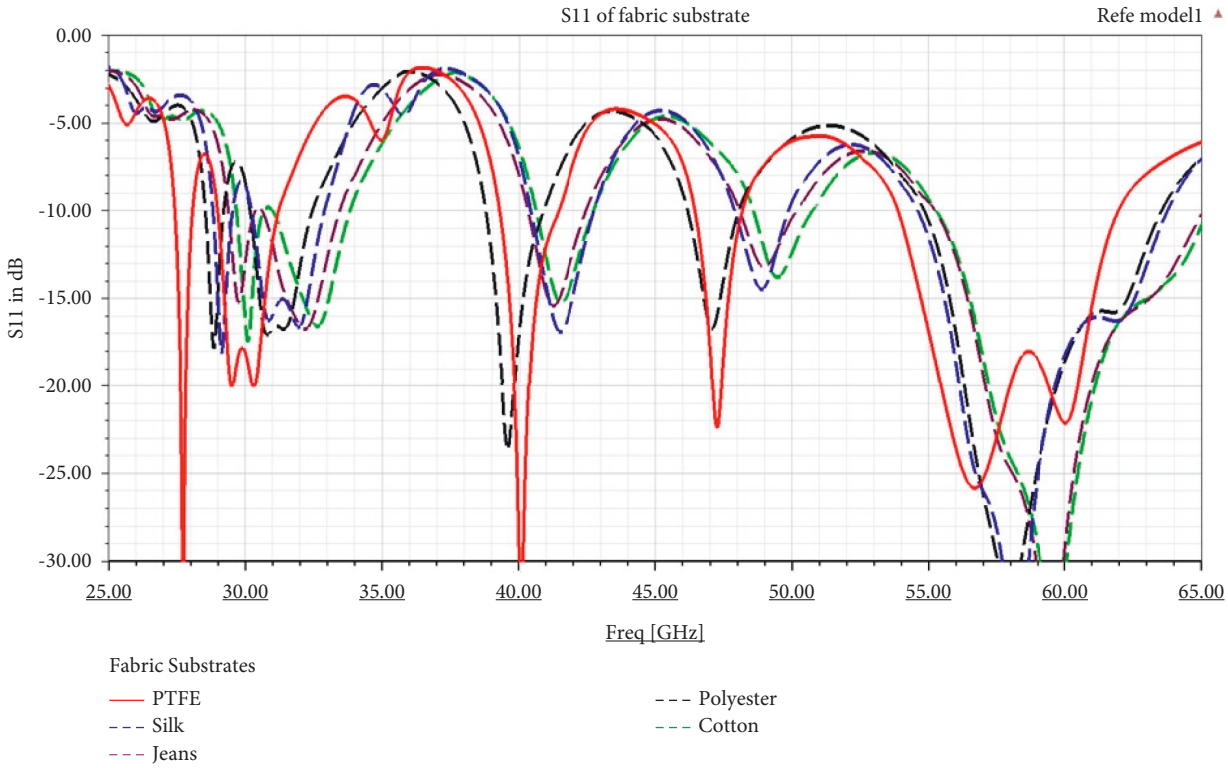

Figure 7: S_{11} result of the genetically optimized antenna with various fabric substrates.

Table 3: The performance of optimized antenna summary at various fabric substrates.

Substrate type	Resonance frequency (GHz)	Peak S_{11} in dB	Peak (dB) directivity	Peak (dB) gain	Bandwidth (GHz)
PTFE	27.8	−34.5	10.3	10.2	0.69
	30.3	−20.1	8.5	8.4	2.32
	40.1	−35.2	7.8	7.7	2.22
	47.2	−22.4	9.6	9.5	1.76
	56.7	−25.8	8.9	8.4	8.11
Silk	29.1	−18.1	9.5	9.3	0.75
	31.9	−16.6	9.6	9.3	2.72
	41.5	−16.9	8.9	8.7	2.35
	48.9	−14.5	8.4	8.2	2.01
	58.2	−38.6	8.3	8.1	9.23
Polyester	28.8	−17.8	8.8	8.7	0.68
	30.8	−17.1	8.7	8.4	2.3
	39.6	−23.6	7.8	7.5	2.12
	47.1	−16.7	8.9	8.7	1.89
	57.9	−32.2	8.8	8.1	8.74
Jeans	29.7	−15.2	9.3	8.9	1.06
	32.2	−16.7	9.4	9.0	3.02
	41.3	−15.4	7.7	7.4	2.16
	49.0	−13.2	9.0	8.9	2.02
	59.5	−38.6	8.7	8.3	9.78
Cotton	30.1	−17.3	9.6	9.1	0.99
	32.6	−16.6	8.9	8.6	2.76
	41.6	−15.2	9.5	9.3	2.22
	49.5	−13.7	8.1	7.8	2.35
	59.6	−34.8	8.8	8.4	9.82

layered phantom that consists of muscle, fat, and skin is designed in HFSS, as shown in Figure 11(a). At 40 GHz, the average permittivity and conductivity of these layers are specified for muscle ($\epsilon_r = 52.79$; $\tan\ \delta = 1.705$), fat ($\epsilon_r = 5.28$; $\tan\ \delta = 0.1$), and skin ($\epsilon_r = 31.29$; $\tan\ \delta = 5.0138$) [28]. In this model, the thickness of muscle, fat, and skin

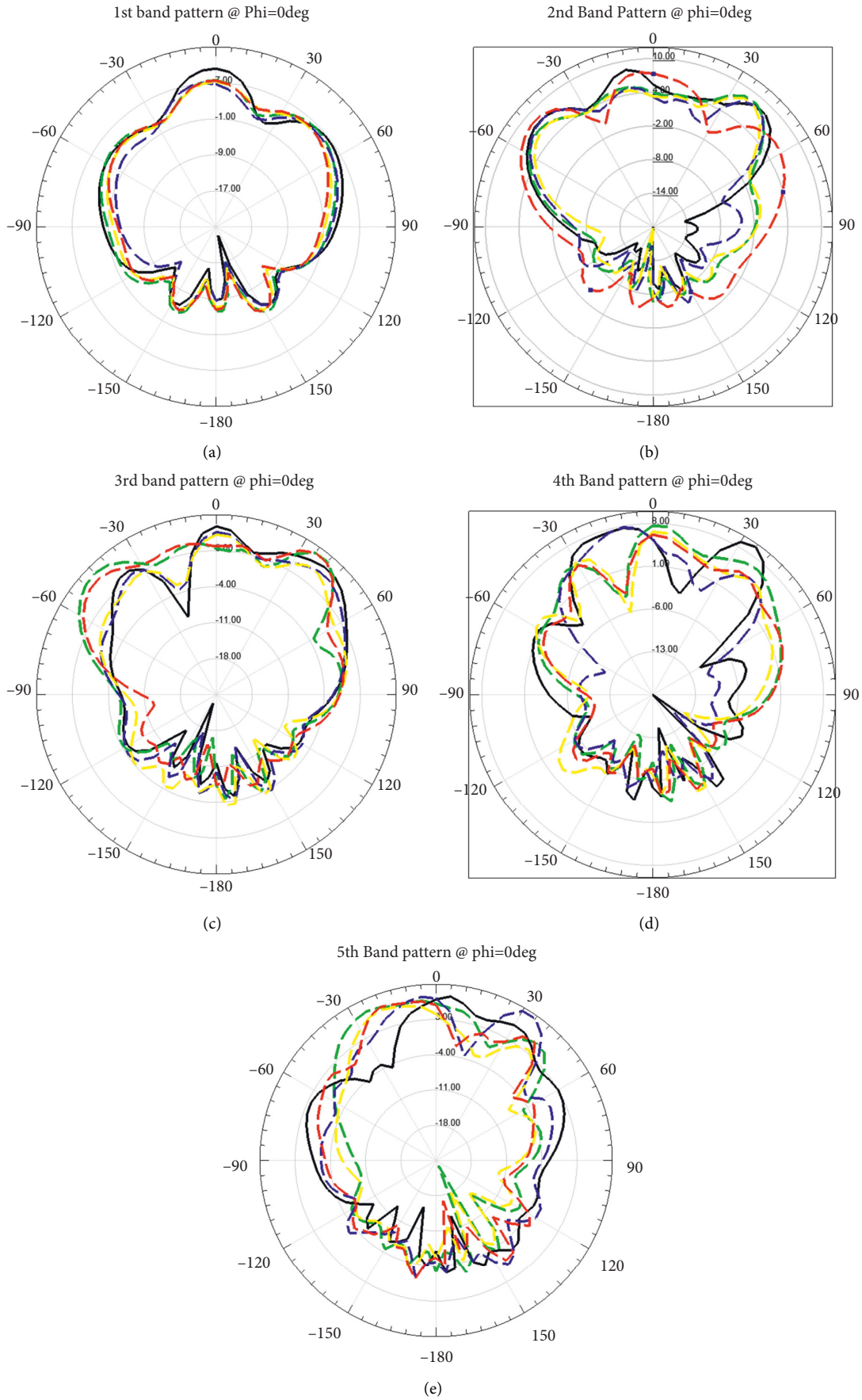

Figure 8: The E-plane gain pattern of the optimized antenna at various fabric substrates.

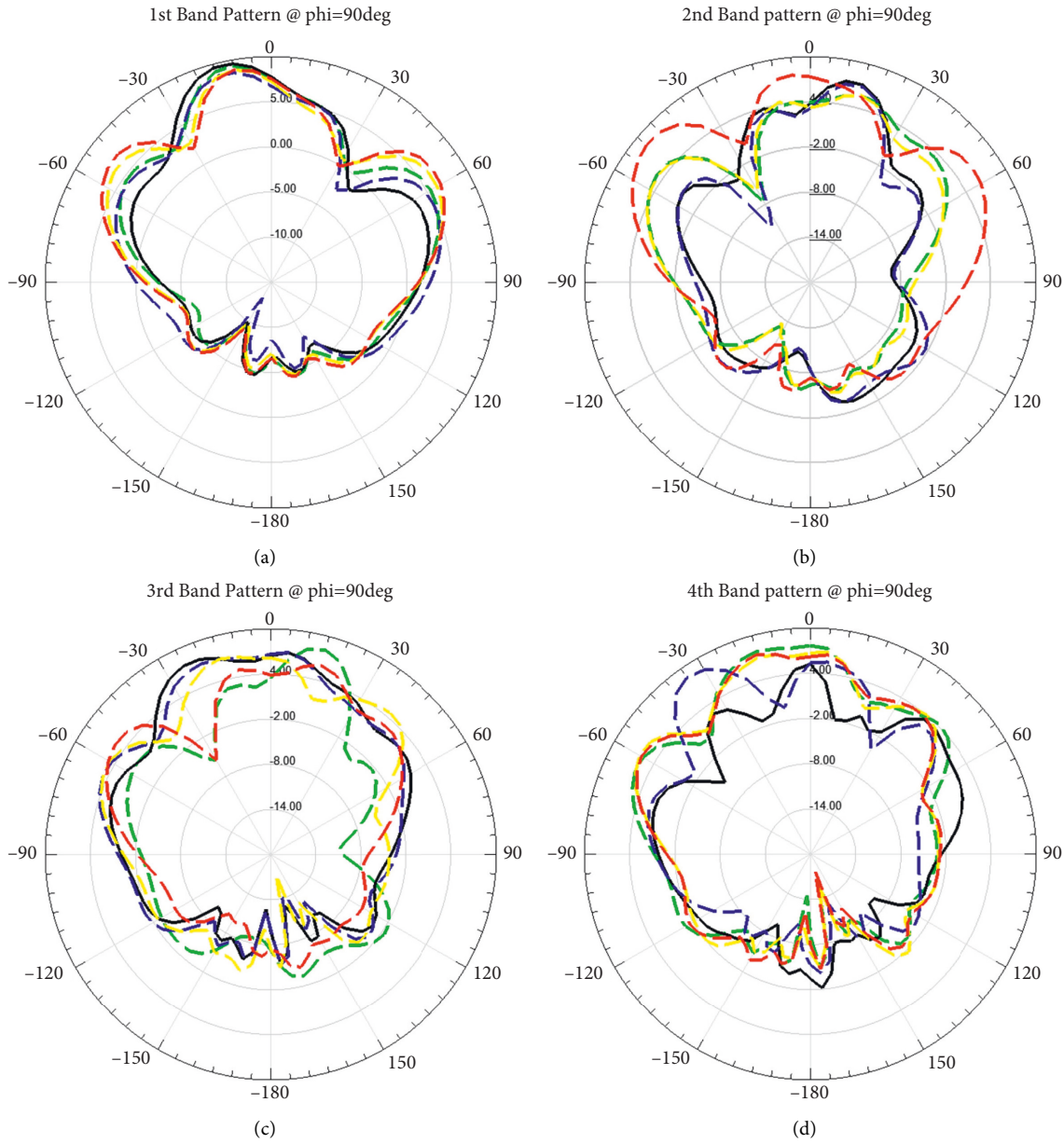

Figure 9: Continued.

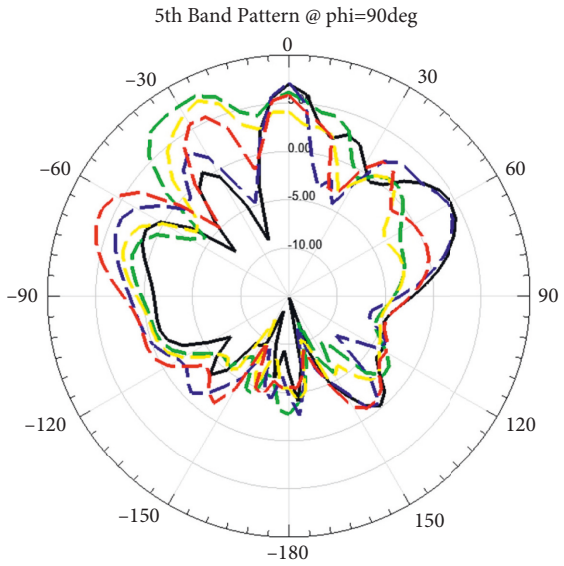

(e)

Figure 9: The H-plane gain pattern of the optimized antenna at various fabric substrates.

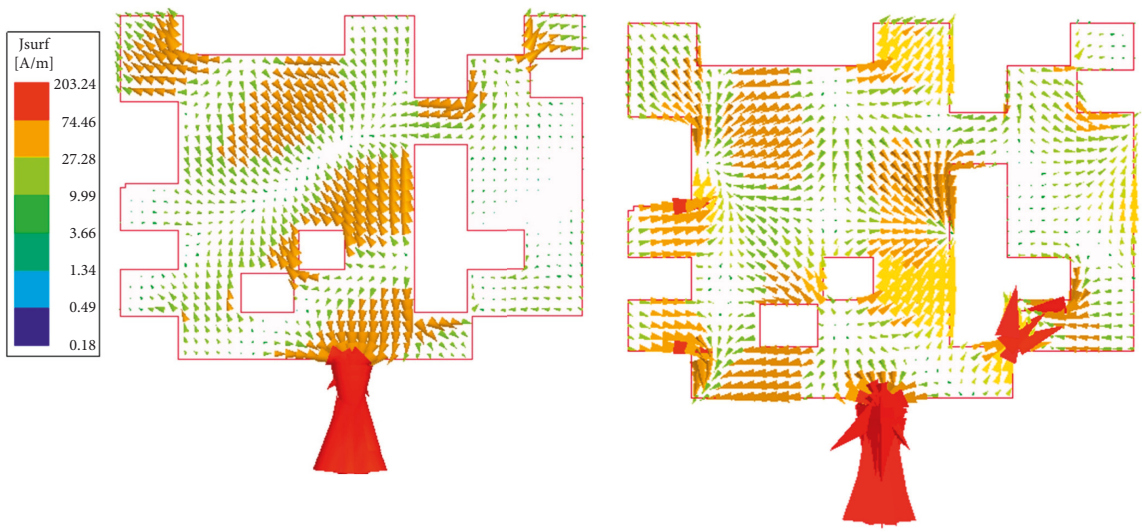

(a) (b)

Figure 10: Continued.

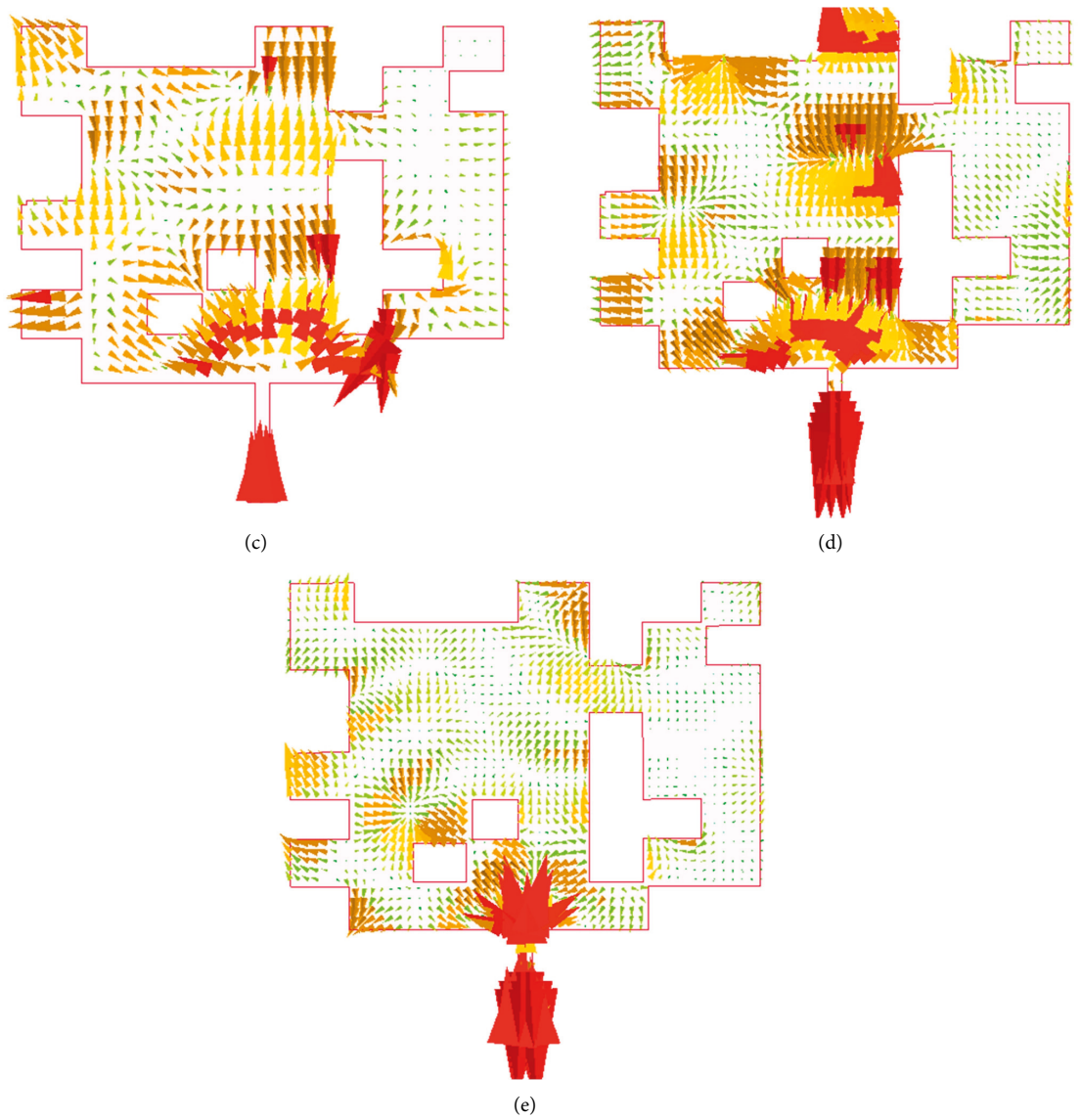

FIGURE 10: Current distribution on the patch surface of the optimized antenna with PTFE substrate at different resonance frequencies: (a) 27.8 GHz, (b) 30.3 GHz, (c) 40.1 GHz, (d) 47.1 GHz, and (e) 56.7 GHz.

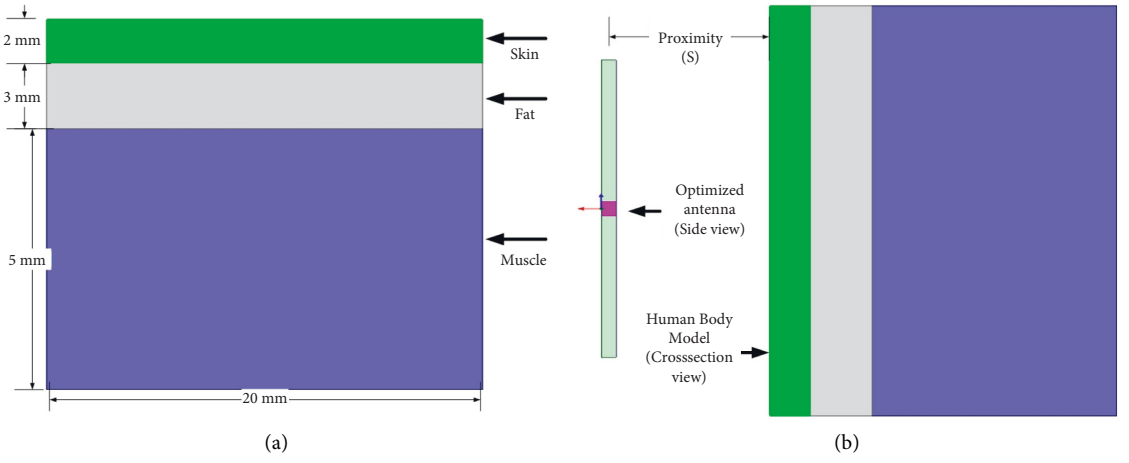

FIGURE 11: (a) Human body model and its dimensions and (b) placement of the optimized antenna in variable proximity (S).

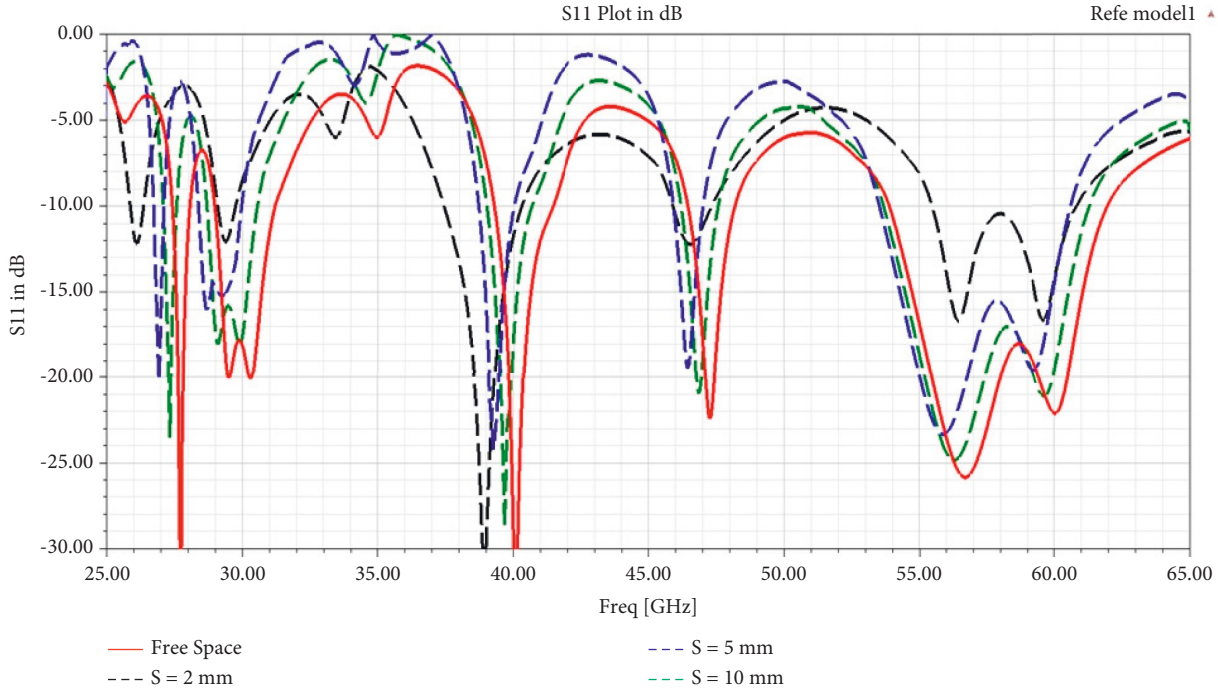

Figure 12: S_{11} performance of the optimized antenna at various proximity from the human model.

Table 4: On-body simulation performance of the optimized antenna at various distances from the body model.

Placement	Resonance frequency (GHz)	Bandwidth (GHz)	Peak (dB) gain	Peak (dB) directivity
On-body, 2 mm	26.1	0.4	5.1	7.4
	29.4	0.8	5.2	7.6
	38.9	2.9	4.8	6.3
	46.6	1.4	4.7	6.5
	56.4	5.4	5.8	8.1
On-body, 5 mm	26.9	0.4	5.8	7.3
	28.7	1.7	5.5	7.1
	39.2	1.3	5.2	6.5
	46.5	1.1	6.0	8.2
	55.9	7	6.2	7.8
On-body, 10 mm	27.3	0.4	6.7	8.0
	29.1	1.9	7.23	8.4
	39.7	1.6	6.1	7.2
	46.8	1.3	8.4	8.9
	56.2	7.6	7.5	8.7
Free space	27.8	0.69	10.2	10.3
	30.3	2.32	8.4	8.5
	40.1	2.22	7.7	7.8
	47.2	1.76	9.5	9.6
	56.7	8.11	8.4	8.9

layers are 5 mm, 3 mm, and 2 mm, respectively. The proposed optimized wearable antenna is fixed on a 20 × 20 × 10 mm flat body phantom to study its radiation characteristics in three proximity levels to the human body. The antenna was positioned at three different distances from the phantom to analyze the antenna performance in wearable scenarios. Starting from 2 mm, the antenna gradually moved away to 10 mm from the phantom. Figures 11(b) show the antenna's position at variable proximity to the model.

Figure 12 shows the S_{11} performance curves of the optimized PTFE substrate antenna corresponding to various proximity placements from the human body model. When the antenna is placed 2 mm, 5 mm, and 10 mm away from the phantom, the center frequency shifts towards lower, as shown in the graph. At the same time, the antenna resonates at five distinct frequencies in each level of proximity. The shifting was not noticeable when the antenna was close to free space at 10 mm proximity. The bandwidth of the optimized antenna was highly affected at 2 mm placement,

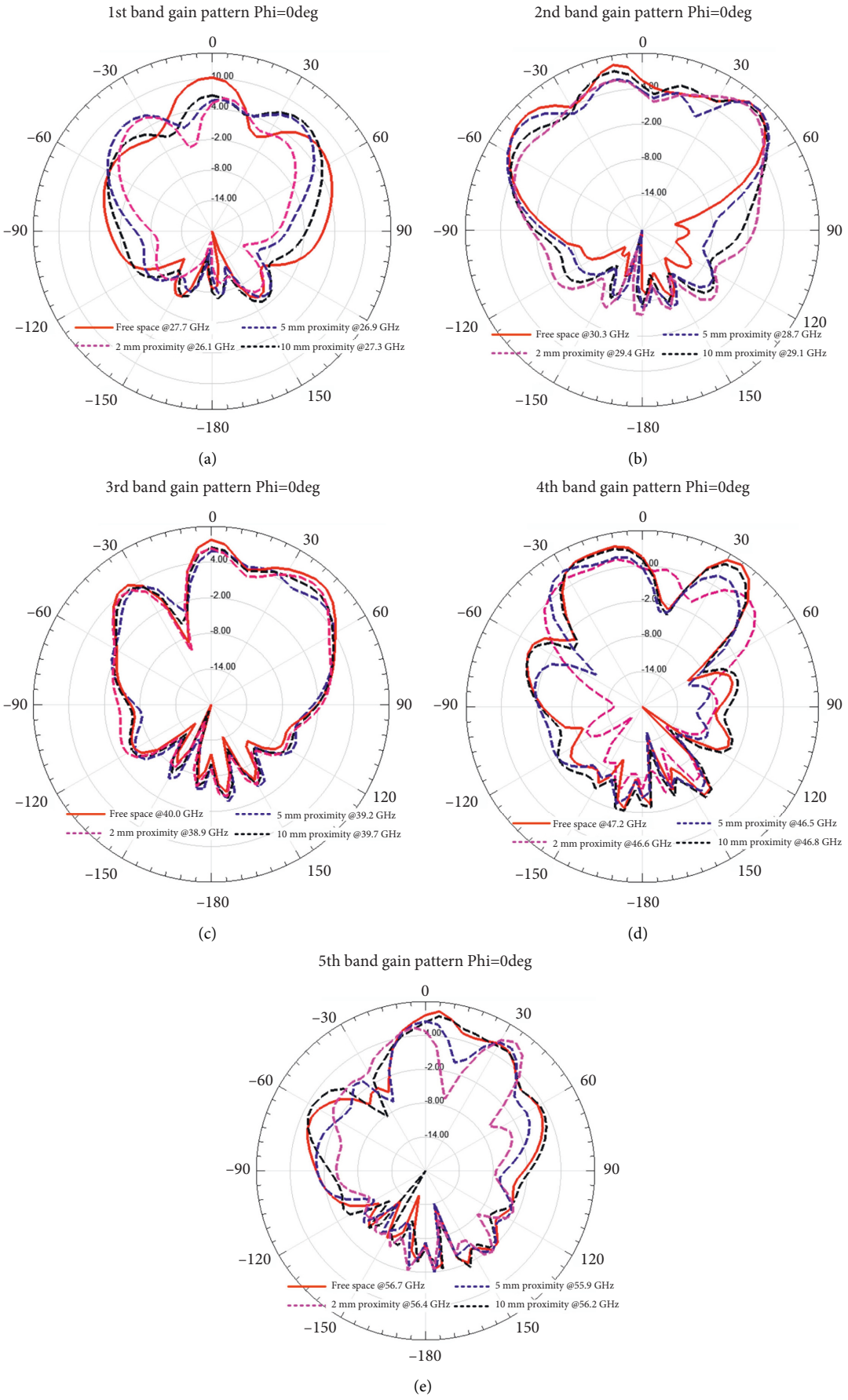

Figure 13: E-plane pattern of optimized antenna at various distances from human body model.

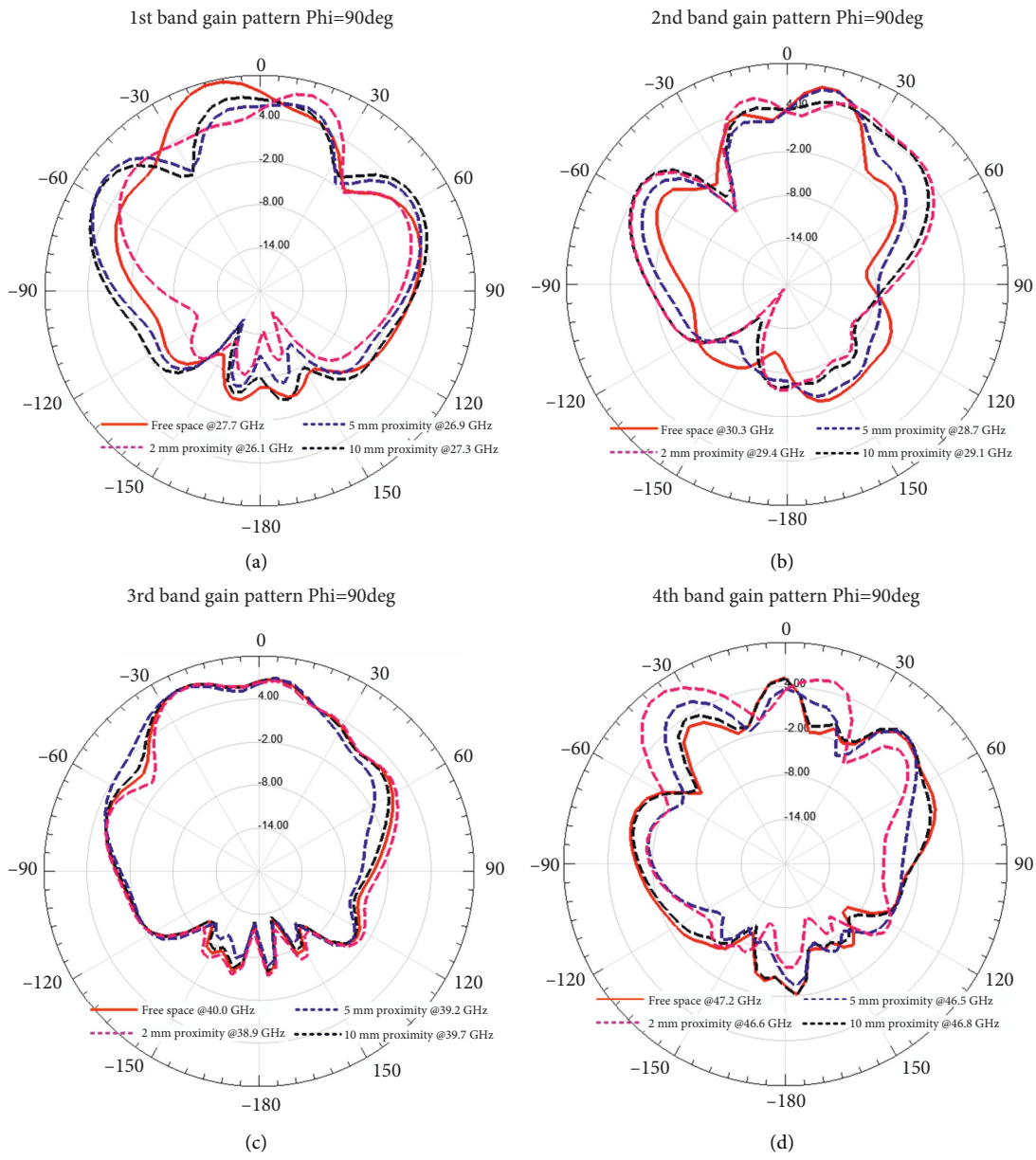

Figure 14: Continued.

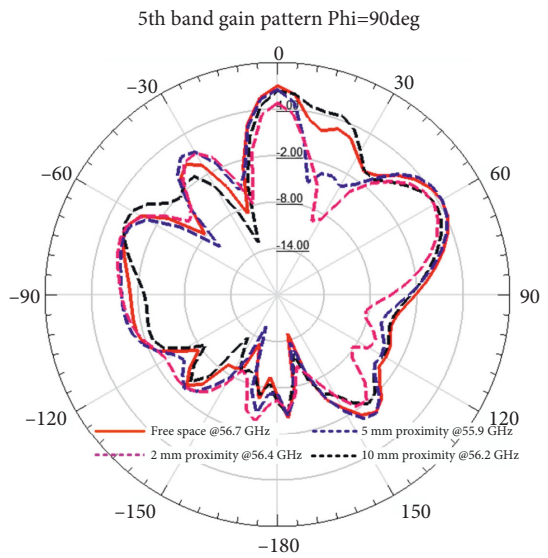

(e)

(e)

Figure 14: H-plane pattern of optimized antenna at various distances from human body model.

Table 5: Performance comparison of this work with similar works in the literature.

Papers	Size of patch (mm)	Resonance frequency (GHz)	Bandwidth (GHz)	Free space gain (dB)	Optimizing method	Material used
[16]	53.6*46	2.403	0.17	5.94	Parametric	Jeans
[27]	11*6.5	60	12.1	8.62	Parametric	FR4 epoxy
[2]	40*34	2.4	0.6	3.8	U-shaped slits	Cotton
[17]	3.36*5.26	28.0 31.1	0.8 0.3	7.5 8.4	Genetic algorithm	RT/duroid 5880 (tm)
[7]	43.2*43.2	5.2 5.8	0.36 0.15	8.0 8.2	Metasurface-based	RO4003
[20]	4.4*6.6	28.0 40.0 47.0	1.8 5.5 0.85	5.64 8.7 6.17	Genetic algorithm	FR4 epoxy
[28]	50 mm diameter	1.8 2.5 3.6 5.8	— — — —	2.5 6 2.6 5.9	Pareto–Estra algorithm	DuPont Pyralux
This paper	14.6*10.8	27.8 30.3 40.1 47.2 56.7	0.69 2.32 2.22 1.76 8.11	10.2 8.4 7.7 9.5 8.4	Genetic algorithm	PTFE

resulting in about 10.9 GHz over all pentaband operations, which is 28% lower than the free space bandwidth coverage.

The gain and radiation efficiency were adversely affected when the antenna operated close to the human body model. When the gap between the antenna and the phantom model gradually increases, radiation efficiency and gain also increase. At a distance of 2 mm, the minimum gain value was observed, which is 4.7 dB. The maximum gain in the on-body simulation was 8.4 dB at 10 mm proximity. However, this value was substantially lower when compared to the free space findings due to the lossy nature of human tissues. Table 4 summarizes the results of the on-body simulation of the optimized antenna with a PTFE substrate. The gain patterns of the antenna in the E-plane and H-plane for various distances are shown in Figures 13 and 14, respectively. The radiation patterns do not change much with multiple antenna placements except for power level variations.

5.4. Comparison with Related Works. Table 5 summarizes the results of genetically improved antennas and some other similar research studies. The originality of this article has

been recognized in terms of its pentaband operation and other performance metrics. For example, in reference [16], a wearable UWB antenna for mm-wave devices was proposed. The antenna was only capable of operating in a single band with a bandwidth of 12.1 GHz. However, this genetically modified wearable antenna can operate in five frequency bands with a total bandwidth of 15.1 GHz. As seen from the comparison table the highest gain was reported by [20], which is 8.7 dB. Nevertheless, the proposed antenna has a maximum gain of 10.2, which indicates its superiority. Aside from the fact that the improved antenna utilizes a flexible textile-based substrate, it also outperforms related works in both free space and on-body simulations, making the optimized antenna a strong choice for wearable devices.

6. Conclusion

This work aimed to optimize and analyze a novel multi-band mm-wave textile-based antenna for wearable applications. A binary-coded genetic algorithm was utilized to optimize the reference patch geometry targeted to enhance the multi-band operation and widen the bandwidth. The improved antenna was simulated in free space and at various distances from a phantom human body model. In free space simulation, the antenna operates in five bands: 27.43–28.12 GHz, 28.94–31.26 GHz, 39.27–41.49 GHz, 46.44–48.2 GHz, and 53.83–61.94 GHz a total bandwidth of 15.11 GHz. The broadside directivity was 10.3, 8.5, 7.8, 9.6, and 8.9 dB in the respective bands. The gain was highly affected when the antenna was close to the human body model compared to free space findings. The antenna was also tested on various flexible textile substrates such as cotton, jeans, silk, and polyester. The finding shows that the antenna has adequate bandwidth coverage in all five distinct bands with sufficient gain. In the future, the performance of the antenna will be tested with moist substrates and different bending angles of the antenna. Due to a lack of adequate laboratory facilities, the paper has only provided simulations at this stage. Therefore, prototype fabrication and measurements will be central to our future work. In summary, the proposed antenna is suitable for multi-band mm-wave wearable devices, and a genetic algorithm based on binary-coded genetic programming could be used to improve the multi-functionality and impedance bandwidth of the antenna.

Data Availability

The data used to support the findings of this study are included within the article.

Conflicts of Interest

The authors declare that they have no conflicts of interest.

References

[1] M. A. Osman, M. K. A. Rahim, N. A. Sassari, M. K. Elbasheer, and M. E. Ali, "Textile UWB antenna bending and wet performances," *International Journal of Antennas and Propagation*, vol. 2012, Article ID 251682, 12 pages, 2012.

[2] S. Karthikeyan, Y. V. Gopal, V. G. N. Kumar, and T. Ravi, "Design and analysis of wearable antenna for wireless body area network," in *Proceedings of the International Conference on Frontiers in Materials and Smart System Technologies*Tamil Nadu, India, IOP Publishing, October 2019.

[3] T. Wu, T. S. Rappaport, and C. M. Collins, "Safe for generations to come: considerations of safety for millimeter waves in wireless communications," *IEEE Microwave Magazine*, vol. 16, no. 2, pp. 65–84, 2015.

[4] Federal Communications Commission Office of Engineering and Technology, *"Millimeter Wave Propagation: Spectrum Management Implications*, Federal Communications Commission, Washington, DC, USA, 1997.

[5] J. Shepard, *Basics of mmWave and its Applications," Analog IC, 21 December 2020*, https://www.analogictips.com/basics-of-mmwave-and-its-applications/, 2020.

[6] S. Albert, "Wideband wearable antennas for 5G, IoT, and medical applications," in *Advanced Radio Frequency Antennas for Modern Communication and Medical Systems*Intech Open, London, Uk, 2020.

[7] G. Mu and P. Ren, "A compact dual-band metasurface-based antenna for wearable medical body-area network devices," *Journal of Electrical and Computer Engineering*, vol. 2020, Article ID 4967198, 10 pages, 2020.

[8] A. Taha, D. Amer Jassim, and H. Hassan Mohammed, "Novel miniaturized folded UWB microstrip antenna-based metamaterial for RF energy harvesting," *International Journal of Communication Systems*, vol. 33, no. 6, Article ID e4305, 2020.

[9] T. Wu, T. S. Rappaport, and C. M. Collins, "The human body and millimeter-wave wireless communication systems: interactions and implications," in *Proceedings of the IEEE International Conference on Communications*London, UK, ICC), 2015.

[10] J. W. Jayasinghe, "Application of genetic algorithm for binary optimization of microstrip antennas: a review," *AIMS Electronics and Electrical Engineering*, vol. 5, no. 4, pp. 315–333, 2021.

[11] J. Kaur, J. Kalsy, and M. V. Kartikeyan, "Subcision plus 50% trichloroacetic acid chemical reconstruction of skin scars in the management of atrophic acne scars: a cost-effective therapy," *Indian Dermatology Online Journal*, vol. 5, no. 1, pp. 95–97, 2014.

[12] C. Jarufe, R. Rodriguez, V. Tapia, and P. Astudillo, "Optimized corrugated tapered slot antenna for mm-Wave applications," *IEEE Transactions on Antennas and Propagation*, vol. 66, no. 3, pp. 1227–1235, 2018.

[13] G. Singh and U. Singh, "Triple band-notched UWB antenna design using a novel hybrid optimization technique based on DE and NMR algorithms," *Expert Systems with Applications*, vol. 184, Article ID 115299, 2021.

[14] B. B. Mangaraj, M. R. Jena, and S. K. Mohanty, "Bacteria foraging algorithm in antenna design," *Applied Computational Intelligence and Soft Computing*, vol. 2016, Article ID 5983469, 11 pages, 2016.

[15] C. N. Hu, P. Lo, C. P. Ho, and D. C. Chang, "Automatic calibration using a modified genetic algorithm for millimeter-wave antenna modules in MIMO systems," *International Journal of Antennas and Propagation*, vol. 2020, Article ID 4286026, 9 pages, 2020.

[16] S. Sankaralingam and B. Gupta, "Determination of dielectric constant of fabric materials and their use as substrates for design and development of antennas for wearable applications," *IEEE Transactions on Instrumentation and Measurement*, vol. 59, no. 12, pp. 3122–3130, 2010.

[17] A. Dejen, J. Jayasinghe, M. Ridwan, and J. Anguera, "Optimization of dual band microstrip mm-wave antenna with improved directivity for mobile application using genetic algorithm," in *Proceedings of the International Conference on Advances of Science and and Technology*, pp. 331–340, Springer, Cham., Bahir Dar, Ethiopia, 2021.

[18] D. E. Goldberg and J. H. Holland, *Genetic Algorithms and Machine Learning*, Addison-Wesley Publishing Company Inc, Boston, USA, 1988.

[19] J. M. J. W. Jayasinghe, J. Anguera, D. N. Uduwawala, and A. Andújar, "High-directivity genetic microstrip patch antenna," *International Journal of Electronics Letters*, vol. 4, no. 3, pp. 279–286, 2016.

[20] A. Dejen, J. Jayasinghe, M. Ridwan, and J. Anguera, "Genetically engineered tri-band microstrip antenna with improved directivity for mm-wave wireless application," *AIMS Electronics and Electrical Engineering*, vol. 6, no. 1, pp. 1–15, 2022.

[21] R. G. Mishra, R. Mishra, P. Kuchhal, and N. P. Kumari, "Optimization and analysis of high gain wideband microstrip patch antenna using genetic algorithm," *International Journal of Engineering and Technology*, vol. 7, no. 1, pp. 176–179, 2018.

[22] M. Lamsalli, A. El Hamichi, and B. Mohamed, "Genetic algorithm optimization for microstrip patch antenna miniaturization," *Progress In Electromagnetics Research Letters*, vol. 60, pp. 113–120, 2016.

[23] B. Almohammed, A. Ismail, and A. Sali, "Electro-textile wearable antennas in wireless body area networks: materials, antenna design, manufacturing techniques, and human body consideration—a review," *Textile Research Journal*, vol. 91, no. 5-6, pp. 646–663, 2021.

[24] C. A. Balanis, *Modern Antenna Handbook*, John Wiley & Sons, Canada, 2013.

[25] J. M. Johnson and Y. Rahmat-samii, "Genetic algorithm optimization and its application to antenna design," in *Proceedings of the IEEE Antennas and Propagation Society International Symposium and URSI National Radio Science Meeting*, Seattle, USA, 1994.

[26] M. Monirujjaman Khan, K. Islam, M. Shovon et al., "Various textiles-based comparative analysis of a millimeter wave miniaturized novel antenna design for body-centric communications," *International Journal of Antennas and Propagation*, vol. 2021, Article ID 2360440, 14 pages, 2021.

[27] A. G. Alharbi, M. M. Khan, K. Islam et al., "Comparative analysis of a super-wideband millimeter wave array antenna for body for body-centric communications," *International Journal of Antennas and Propagation*, vol. 2022, Article ID 6963284, 21 pages, 2022.

[28] M. M. Khan, J. Hossain, K. Islam et al., "Design and study of an mm Wave wearable textile based compact antenna for healthcare applications," *International Journal of Antennas and Propagation*, vol. 2021, Article ID 6506128, 17 pages, 2021.

[29] M. M. Khan, K. Islam, A. Shovon, M. Nakib, M. Baz, and M. Masud, "Design of a novel 60 GHz millimeter wave Q-slot antenna for body-centric communications," *International Journal of Antennas and Propagation*, vol. 2021, no. Nov 2, 12 pages, Article ID 9795959, 2021.

[30] L. Januszkiewicz, P. D. Barba, and J. Kawecki, "Design optimization of wearable multiband Antenna using evolutionary algorithm tuned with dipole benchmark problem," *MDPI Electronics*, vol. 10, no. 18, pp. 22–49, 2021.

[31] T. A. Elwi and A. M. Al-Saegh, "Further realization of a flexible metamaterial-based antenna on indium nickel oxide polymerized palm fiber substrates for RF energy harvesting," *International Journal of Microwave and Wireless Technologies*, vol. 13, no. 1, pp. 67–75, 2020.